



The following Communications have been judged by at least two referees to be “very important papers” and will be published online at www.angewandte.org soon:

M. A. Newton, M. Di Michiel, A. Kubacka, A. Iglesias-Juez, M. Fernández-García

Observing Oxygen Storage and Release at Work under Cycling Redox Conditions: Synergies between Noble Metal and Oxide Promoter

P. Berrouard, A. Najari, A. Pron, D. Gendron, P.-O. Morin, J.-R. Pouliot, J. Veilleux, M. Leclerc*

Synthesis of 5-Alkyl[3,4- ϵ]thienopyrrole-4,6-dione-Based Polymers through Direct Heteroarylation

J. Zeng, C. Zhu, J. Tao, M. Jin, H. Zhang, Z.-Y. Li, Y. Zhu, Y. Xia*
Controlling the Nucleation and Growth of Silver on Palladium Nanocubes by Manipulating the Reaction Kinetics

C. A. DeForest, K. S. Anseth*

Photoreversible Patterning of Biomolecules within Click-Based Hydrogels

T. A. Nigst, J. Ammer, H. Mayr*

Ambident Reactivities of Methylhydrazines

M. Nazaré,* H. Matter,* D. W. Will, M. Wagner, M. Urmann, J. Czech, H. Schreuder, A. Bauer, K. Ritter, V. Wehner

Fragment Deconstruction of Small, Potent Factor Xa Inhibitors: Exploring the Superadditivity Energetics of Fragment Linking in Protein–Ligand Complexes

G. J. L. Bernardes, G. Casi, S. Trüssel, I. Hartmann, K. Schwager, J. Scheuermann, D. Neri*

A Traceless Vascular Targeting Antibody–Drug Conjugate for Cancer Therapy

H. Chinen, K. Mawatari, Y. Pihosh, K. Morikawa, Y. Kazoe, T. Tsukahara, T. Kitamori*

Enhancement of Proton Mobility in Extended Nanospace Channels

K. Mandal, B. L. Pentelute, D. Bang, Z. P. Gates, V. Y. Torbeev, S. B. H. Kent*

Design, Total Chemical Synthesis, and X-ray Structure of a Protein with a Novel Polypeptide Chain Topology



“The most important thing I learned from my parents is ‘persistence is power’.

My favorite place on earth is Hawaii ...”

This and more about Keiji Maruoka can be found on page 580.

Author Profile

Keiji Maruoka _____ 580–581



S. Shaik



I. Marek



Y. Apeloig



K. Maruoka

News

Frontiers in Biological Chemistry
Lectureship: S. Shaik _____ 582

RSC Organometallic Award:
I. Marek _____ 582

Order of Merit:
Y. Apeloig _____ 582

And also in the News ... _____ 582

Books

Biomimetic Organic Synthesis

Erwan Poupon, Bastien Nay

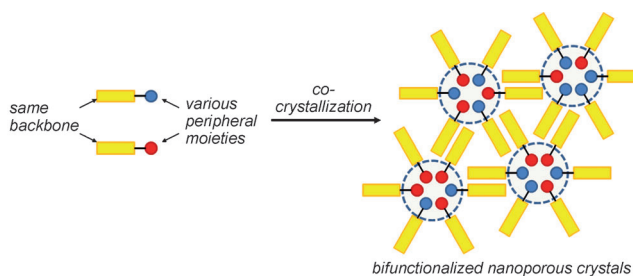
reviewed by M. Kalesse _____ 583

Highlights

Porous Organic Crystals

M. Mastalerz* ————— 584 – 586

Rational Design of Multifunctional Nanopores by Mixing Matching Molecules



Alloying allowed: The self-assembling motifs of rigid steroid molecules (see scheme, left) into nanoporous crystals allows the combination of functional

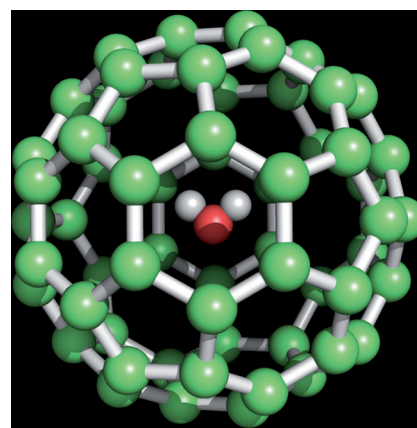
groups (shown in red and blue) inside the pores of binary, ternary, and quaternary co-crystals, resulting multifunctional porous materials.

Endohedral Fullerene

C. Thilgen* ————— 587 – 589

A Single Water Molecule Trapped Inside Hydrophobic C₆₀

Dry water in a wet dungeon? An isolated H₂O molecule has been trapped permanently inside hydrophobic C₆₀ (see picture; green C, white H, red O). The endohedral fullerene H₂O@C₆₀ was synthesized by opening, filling, and reclosing the carbon cage. The incarcerated water does not alter the structure of the cage, but it confers an appreciable dipole moment to the new entity with its intrinsically apolar carbon sphere.



Essays

Symbolism of Arrows

S. Alvarez* ————— 590 – 600



Chemistry: A Panoply of Arrows



Alchemists incorporated arrows in their symbolism (see picture) hundreds of years before modern chemists adopted arrows in chemical equations. The next time you insert an arrow in a chemical text

consider why precisely that arrow is needed. What does it really mean? How did we learn to use arrows in chemistry? What do our arrows have in common with those of abstract artists?

For the USA and Canada: ANGEWANDTE CHEMIE International Edition (ISSN 1433-7851) is published weekly by Wiley-VCH, PO Box 191161, 69451 Weinheim, Germany. Air freight and mailing in the USA by Publications Expediting Inc., 200 Meacham Ave., Elmont, NY 11003. Periodicals

postage paid at Jamaica, NY 11431. US POSTMASTER: send address changes to *Angewandte Chemie*, Journal Customer Services, John Wiley & Sons Inc., 350 Main St., Malden, MA 02148-5020. Annual subscription price for institutions: US\$ 11.738/10.206 (valid for print and electronic / print or electronic delivery); for

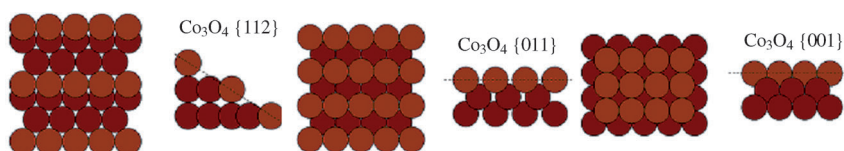
individuals who are personal members of a national chemical society prices are available on request. Postage and handling charges included. All prices are subject to local VAT/sales tax.

Minireviews

Heterogeneous Catalysis

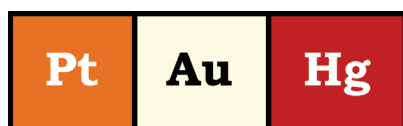
K. B. Zhou, Y. D. Li* _____ 602–613

Catalysis Based on Nanocrystals with Well-Defined Facets



Shape-controlled nanocrystals (NCs) are a new frontier in heterogeneous catalysis. Research into these NCs has shown that the catalytic properties of a material are sensitive not only to the size but also to

the shape of the NCs owing to well-defined facets. Shape-controlled NCs may serve to bridge the gap between model surfaces and real catalysts.



Relatively related: Relativistic effects in the valence shell of the chemical elements reach a maximum in the triad Pt–Au–Hg and influence their catalytic activity in organic reactions. The catalytic activity for some representative reactions is examined together with other relevant properties, such as toxicity, price, and availability. For the reactions considered, gold is generally preferred to mercury or platinum catalysts.

Reviews

Metal Catalysis

A. Leyva-Pérez, A. Corma* _____ 614–635

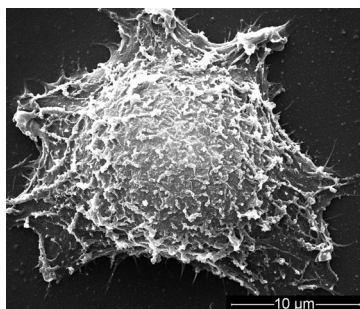
Similarities and Differences between the “Relativistic” Triad Gold, Platinum, and Mercury in Catalysis

Communications

Gold Nanorods

L. Vigderman, P. Manna, E. R. Zubarev* _____ 636–641

Quantitative Replacement of Cetyl Trimethylammonium Bromide by Cationic Thiol Ligands on the Surface of Gold Nanorods and Their Extremely Large Uptake by Cancer Cells



Stable and biocompatible: The chemical composition of synthesized cationic thiolate-monolayer-protected gold nanorods was precisely determined. In vitro cell culture experiments showed no cytotoxicity of these nanorods, and the number of nanorods that were taken up by each cancer cell exceeded two million particles (see picture).

Frontispiece

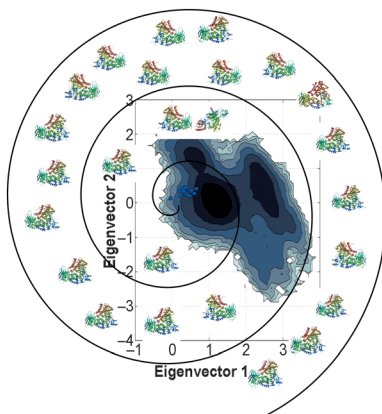


Computational Chemistry

M. D'Abramo, O. Rabal, J. Oyarzabal,*
F. L. Gervasio* _____ 642–646



Conformational Selection versus Induced Fit in Kinases: The Case of PI3K- γ



Kinase binding: The mechanism of molecular recognition in the pharmacologically relevant phosphoinositide 3-kinase PI3K- γ has been investigated. The analysis of molecular dynamics simulations, free energy calculations, and docking interactions suggests that a combination of two proposed limiting mechanisms, conformational selection and induced fit, may best explain binding events between the ligand and its target.

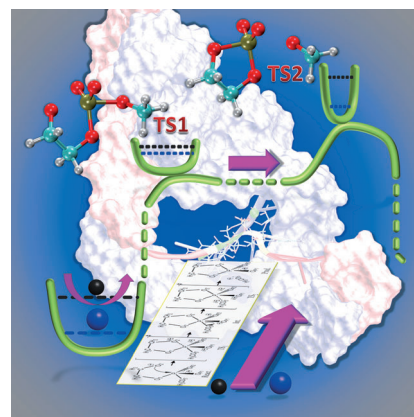
Reaction Mechanisms

K.-Y. Wong,* H. Gu, S. Zhang,
J. A. Piccirilli,* M. E. Harris,*
D. M. York* _____ 647–651



Characterization of the Reaction Path and Transition States for RNA Transphosphorylation Models from Theory and Experiment

Model behavior: The primary and secondary kinetic isotope effects for a model compound which represents RNA cleavage transesterification were calculated and compared with experimental measurements. Based on the good agreement between theory and experiments, the energy profile, reaction pathway, and two distinct transition states for the reactions of the model compound and two thio-substituted analogues were characterized (see scheme).



Inside Back Cover

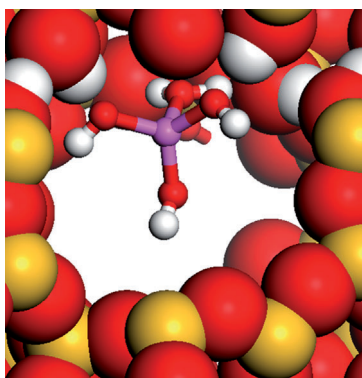


Zeolites

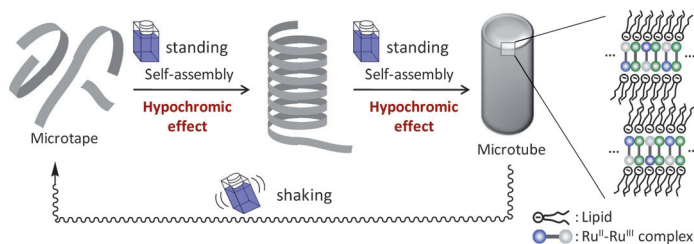
S. Malola, S. Svelle, F. L. Bleken,
O. Swang* _____ 652–655



Detailed Reaction Paths for Zeolite Dealumination and Desilication From Density Functional Calculations



Birth of a silanol nest: Reaction paths for the extraction of Al and Si from zeolites by reaction with steam were investigated by first-principles DFT calculations. The results show that dealumination is energetically favored over desilication (see picture: O red, Si yellow, Al purple, H white).



Mix and shake: Lipid packaged dinuclear ruthenium(II,III) complexes of class III mixed-valence state produce a reversible hypochromic effect upon external physical stimuli, such as shaking, due to the

arrangement of transition dipole moments. The effect is accompanied by tubular-to-ribbon structural changes (see scheme).

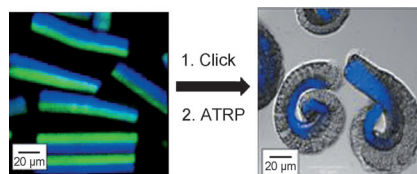
Supramolecular Chemistry

K. Kuroiwa,* M. Yoshida, S. Masaoka,*
K. Kaneko, K. Sakai,
N. Kimizuka _____ **656–659**

Self-Assembly of Tubular Microstructures from Mixed-Valence Metal Complexes and Their Reversible Transformation by External Stimuli



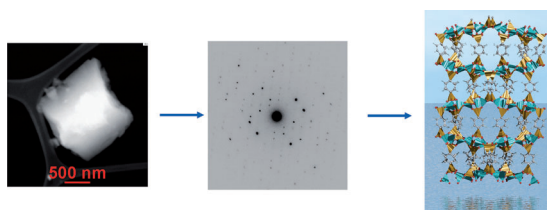
The bends: Surface modification of multi-compartmental microcylinders by spatio-selective click chemistry and subsequent surface-initiated atom-transfer radical polymerization (ATRP) yield novel amphiphilic microcylinders (see scheme). Depending on the aspect ratio of the microcylinders, they can be bent or coiled.



Anisotropic Materials

S. Saha, D. Copic, S. Bhaskar, N. Clay,
A. Donini, A. J. Hart,
J. Lahann* _____ **660–665**

Chemically Controlled Bending of Compositionally Anisotropic Microcylinders



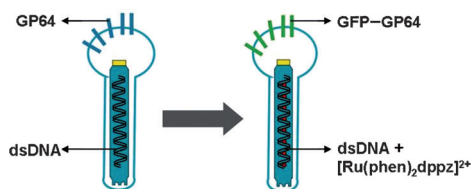
Automated diffraction tomography was used to collect electron-diffraction data for solving the crystal structure of ECS-3, which is the first example of a crystalline hybrid organic–inorganic aluminosilicate

with open porosity, generated by a regular arrangement of phenylene rings interconnecting aluminosilicate layers (see picture; Al turquoise, C gray, O red, Si gold).

Hybrid Materials

G. Bellussi, E. Montanari, E. Di Paola,
R. Millini, A. Carati, C. Rizzo,
W. O'Neil Parker, Jr., M. Gemmi,
E. Mugnaioli, U. Kolb,
S. Zanardi* _____ **666–669**

ECS-3: A Crystalline Hybrid Organic–Inorganic Aluminosilicate with Open Porosity



Dual-color virus particles were obtained by labeling a glycoprotein (GP64) on the surface of a baculovirus with a green fluorescent protein (GFP) and labeling the nucleic acid (dsDNA) at the same time

with the red fluorescent $[\text{Ru}(\text{phen})_2\text{-}(\text{dppz})]^{2+}$ complex during the viral replication in host cells, by using an in vivo virus self-assembly system. This labeling strategy does not affect the viral infectivity.

Virus Labeling

P. Zhou, Z. Zheng, W. Lu, F. Zhang,
Z. Zhang, D. Pang, B. Hu, Z. He,*
H. Wang* _____ **670–674**

Multicolor Labeling of Living-Virus Particles in Live Cells



Nanostructures

B. J. Kim, Y. S. Choi, H. J. Cha* 675–678

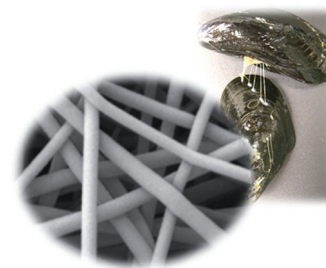


Reinforced Multifunctionalized Nanofibrous Scaffolds Using Mussel Adhesive Proteins



Back Cover

Sticky stuff: The novel composite nanofibrous scaffolds based on mussel adhesive proteins (MAPs) provide a mechanically durable structural backbone with the function of bioactive peptides. It can also be easily coated with a variety of biomolecules. This biofunctionalized nanofiber platform could be a promising tool for successful tissue-engineering applications.



MAP-based composite nanofibrous scaffolds

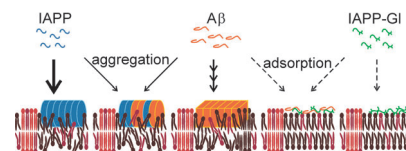
Amyloid–Peptide Interactions

J. Seeliger, F. Evers, C. Jeworrek, S. Kapoor, K. Weise, E. Andreetto, M. Tolan, A. Kapurniotu, R. Winter* 679–683



Cross-Amyloid Interaction of A β and IAPP at Lipid Membranes

Membrane controlled protein assembly: A study of the amyloid interaction of the islet amyloid polypeptide (IAPP), β -amyloid (A β), and a mixture of both with an anionic model raft membrane showed the dominant effect of IAPP on the aggregation process and on the hydrogen-bonding pattern of the assemblies present in the mixture (see picture). The analysis of the interaction of A β with IAPP-GI—a non-amyloidogenic IAPP mimic—confirmed these findings.

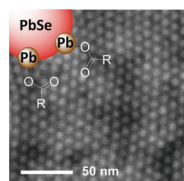


Nanocrystals

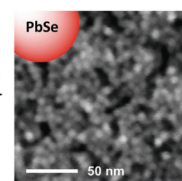
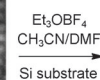
E. L. Rosen, R. Buonsanti, A. Llordes, A. M. Sawvel, D. J. Milliron, B. A. Helms* 684–689



Exceptionally Mild Reactive Stripping of Native Ligands from Nanocrystal Surfaces by Using Meerwein's Salt



PbSe-Oleate
insulating



Bare PbSe
no particle etching
increase in conductivity

Ole-ain't: Trialkyl oxonium salts are universal reagents for native-ligand stripping of carboxylate- (e.g., oleate-), phosphate-, and amine-passivated nanocrystal thin films and dispersions to give bare or BF₄⁻/DMF-passivated surfaces. Meer-

wein-activated PbSe nanocrystal thin films (see picture) show hole mobilities of about 2–4 cm²V⁻¹s⁻¹, which suggest applications of this process in fabricating high-performance devices.

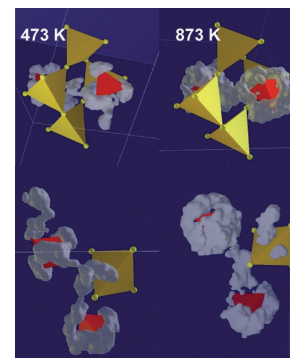
Oxide Ion Conductors

X. Kuang, J. L. Payne, M. R. Johnson, I. Radosavljevic Evans* 690–694

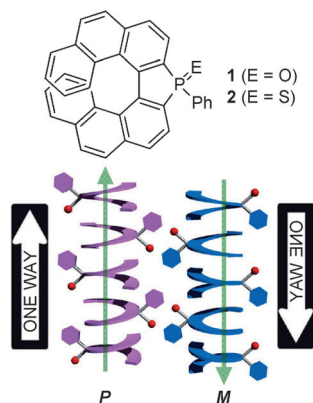


Remarkably High Oxide Ion Conductivity at Low Temperature in an Ordered Fluorite-Type Superstructure

Mobile oxide ions: A remarkably high oxide ion conductivity at low temperatures has been found in an ordered δ -Bi₂O₃ superstructure with the composition Bi_{1-x}V_xO_{1.5+x} ($x=0.087$ and 0.095), and attributed to a combination of highly polarizable sublattice with vacancies, central atoms able to support variable coordination numbers and geometries, as well as rotational flexibility of these coordination polyhedra, co-existing in a pseudo-cubic structure (see picture).



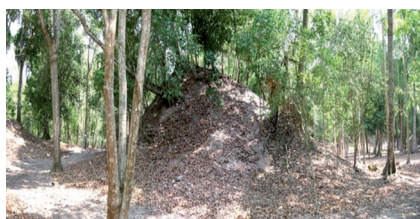
One-way street: A new family of λ^5 -phospha[7]helicenes which form one-dimensional columnar stacks in the solid state were synthesized (see scheme). Neighboring stacks have opposite dipole directions and, in the case of the racemic phosphole sulfide based helicene, columns with a given dipole direction consist of one enantiomer, whereas columns with the opposite dipole direction consist of the other enantiomer.



Heterocyclic Chemistry

K. Nakano, H. Oyama, Y. Nishimura,
S. Nakasako, K. Nozaki — 695–699

λ^5 -Phospha[7]helicenes: Synthesis,
Properties, and Columnar Aggregation
with One-Way Chirality



Historic chemistry: The discovery of a set of greenish pellets from ancient plaster at the La Blanca archaeological site (Guatemala) provides evidence that the Maya people used a material akin to Maya Blue also outside of pottery, murals, sculptures or religious context. Obviously, the Maya people developed different preparative strategies to obtain inorganic–organic hybrid materials.

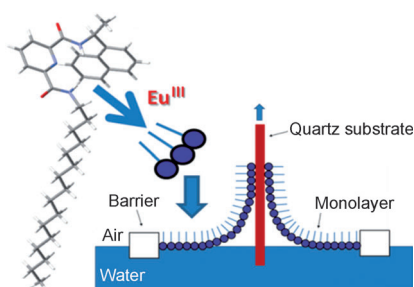
Historical Pigments

A. Doménech,* M. T. Doménech-Carbó,
C. Vidal-Lorenzo,
M. L. V. de Agredos-Pascual — 700–703

Insights into the Maya Blue Technology:
Greenish Pellets from the Ancient City of
La Blanca



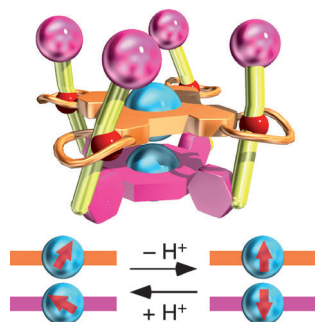
Europium union: The development of chiral amphiphilic self-assembled complexes by europium(III)-directed synthesis is described. These systems form stable Langmuir–Blodgett (LB) films on quartz slides to give stable monolayers that exhibit the first example of time-delayed Eu^{III} -centered emission and circularly polarized luminescence (CPL) from an LB film.



Lanthanides

J. A. Kitchen,* D. E. Barry, L. Mercs,
M. Albrecht, R. D. Peacock,
T. Gunnlaugsson* — 704–708

Circularly Polarized Lanthanide
Luminescence from Langmuir–Blodgett
Films Formed from Optically Active and
Amphiphilic Eu^{III} -Based Self-Assembly
Complexes



Firmly tied: A four-fold rotaxane was prepared from a porphyrin unit with four alkyllammonium chains and a phthalocyanine unit with four peripheral crown ethers. In a dinuclear Cu^{2+} complex of the four-fold rotaxane, the Cu^{2+} –porphyrin and the Cu^{2+} –phthalocyanine moieties were stacked efficiently on one another to afford spin–spin communication. The spin states were switched reversibly (see picture).

Rotaxanes

Y. Yamada, M. Okamoto, K. Furukawa,
T. Kato, K. Tanaka* — 709–713

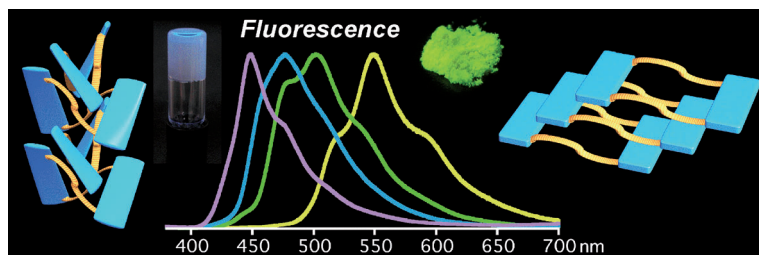
Switchable Intermolecular
Communication in a Four-Fold Rotaxane



π -Aggregation Control

S. Saito, K. Nakakura,
S. Yamaguchi* — 714–717

Macrocyclic Restriction with Flexible Alkylene Linkers: A Simple Strategy to Control the Solid-State Properties of π -Conjugated Systems



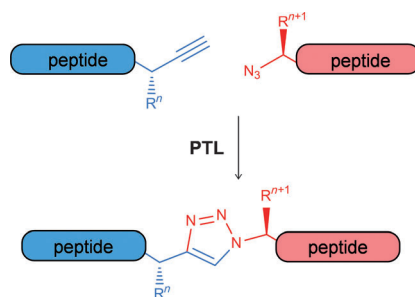
Cyclic and flexible: A simple molecular design for controlling the packing structure and solid-state properties of π -conjugated skeletons is proposed. A subtle difference of the flexible alkylene linker

chain lengths of cyclic terthiophene dimers leads to distinct packing structures, and accordingly the solid-state properties, such as the gelation ability and photophysical properties.

Protein Chemical Synthesis

I. E. Valverde, F. Lecaille, G. Lalmanach,
V. Aucagne,* A. F. Delmas* — 718–722

Synthesis of a Biologically Active Triazole-Containing Analogue of Cystatin A Through Successive Peptidomimetic Alkyne–Azide Ligations

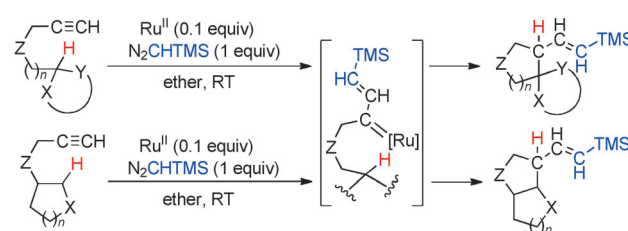


“Click” protein: Cu^I-catalyzed cycloaddition of azides and terminal alkynes has been applied to the successive ligations of three unprotected peptide fragments. Peptidomimetic triazole ligation (PTL, see scheme) as a new method for the chemical production of bioactive proteins is applied for the synthesis of a triazole-containing analogue of the 97 amino acid protein cystatin A.

Homogeneous Catalysis

F. Cambeiro, S. López, J. A. Varela,
C. Saá* — 723–727

Cyclization by Catalytic Ruthenium Carbene Insertion into C_{sp³}–H Bonds



A novel tandem Ru-catalyzed carbene addition to terminal alkynes/insertion into C_{sp³}–H bonds in alkyne acetals, ethers, and amines has been accomplished under mild reaction conditions (see scheme; TMS = trimethylsilyl). This cascade pro-

vides an efficient approach to form complex spiro and fused bicyclic structures by 1,5- and 1,6-hydride shift/cyclization sequences from vinylcarbene Ru intermediates.

Natural Product Synthesis

K. C. Nicolaou,* D. Giguère,
S. Totokotsopoulos, Y.-P. Sun — 728–732

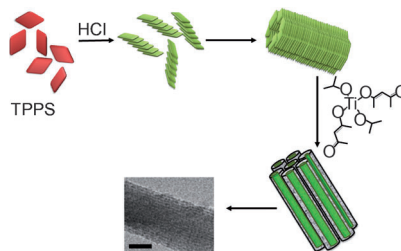
A Practical Sulfenylation of 2,5-Diketopiperazines



Sulfurs in action: A practical and simple method has been developed for the introduction of sulfur atoms into 2,5-diketopiperazines (I) under mild condi-

tions. The reaction provides more or less complex epithiodiketopiperazines (II) and bis-methylthiodiketopiperazines (III).

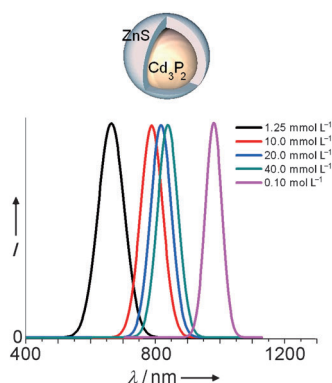
Enveloping porphyrin arrays: Supramolecular arrays of self-assembled tetrakis(4-sulfonatophenyl)porphyrin (TPPS) molecules have been enveloped with an ultrathin layer of titanium dioxide (see picture; scale bar: 25 nm). Integration of the hybrid components at close-to-molecular dimensions preserves optical and chiral properties of J-aggregate superstructures but also enhances photocatalytic activity of TiO₂.



Hybrid Materials

A. J. Patil,* Y. C. Lee, J. W. Yang,
 S. Mann* _____ 733–737

Mesoscale Integration in Titania/J-
 Aggregate Hybrid Nanofibers



By designing highly soluble precursors, Cd₃P₂/ZnS quantum dots (QDs) can be prepared at room temperature. They are shown to be air-stable, size-tunable, and of high optical quality (quantum yields over 50%). A large photoluminescence range can be covered by simple modulation of the concentration of reactants (see picture) and of the temperature (30 °C, 90 °C).

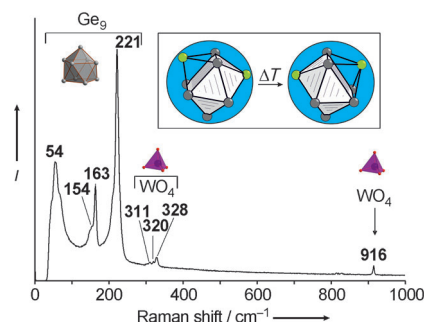
Quantum-Dot Synthesis

W.-S. Ojo, S. Xu, F. Delpech,* C. Nayral,*
 B. Chaudret _____ 738–741

Room-Temperature Synthesis of Air-
 Stable and Size-Tunable Luminescent
 ZnS-Coated Cd₃P₂ Nanocrystals with High
 Quantum Yields



Crystal engineering: The syntheses, crystal structures, Raman spectra, and thermal properties of Cs₁₀[Ge₉]₂[WO₄] and Cs₁₁[Ge₉]₂[VO₄] containing [Ge₉]⁴⁻ clusters and oxometallate anions [MO₄]^{x-} (M = W and V) are reported. The picture shows a Raman spectrum obtained from single crystals of the double salt Cs₁₀[Ge₉]₂[WO₄] as well as the temperature-dependent Ge₉ cluster relocation in Cs₁₁[Ge₉]₂[VO₄].



Solid-State Chemistry

V. Hlukhyy, T. F. Fässler* _____ 742–747

At the Border of Intermetallic Compounds
 and Transition-Metal Oxides: Crystal
 Intergrowth of the Zintl Phase Cs₄Ge₉ and
 Cs₂WO₄ or Cs₃VO₄ as well as Nine-Atom
 Cluster Relocation in the Solid State



Touchscreen testing: A biomolecular detection platform is presented that utilizes a capacitive touchscreen to measure DNA concentration. The technology is ready for integration into touchscreen-equipped smart phones or smart pads, and should truly accelerate the realization of personalized portable biosensors.

Biosensors

B. Y. Won, H. G. Park* _____ 748–751

A Touchscreen as a Biomolecule
 Detection Platform

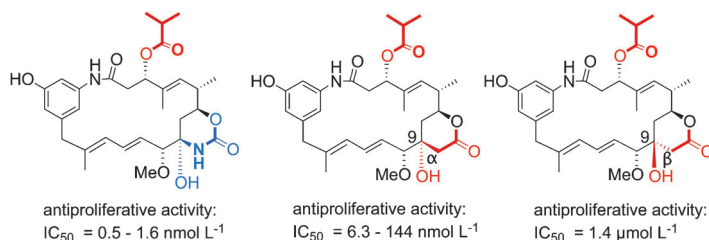


Inside Cover



Natural Products

S. Eichner, T. Knobloch, H. G. Floss, J. Fohrer, K. Harmrolfs, J. Hermane, A. Schulz, F. Sasse, P. Spittler, F. Taft, A. Kirschning* _____ 752–757



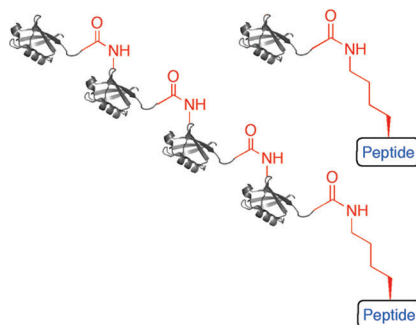
The Interplay between Mutasynthesis and Semisynthesis: Generation and Evaluation of an Ansamitocin Library

Working hand in hand! The synthetic power of three mutant strains that produce ansamitocin and geldanamycin is combined with chemical synthesis, thus leading to 27 new ansamitocin derivatives. Structure–activity studies show that

the N of the carbinolamide moiety is not important for cytotoxic activity but the α orientation of the OH group at C9 is key [see structures; chemical synthesis (red), mutasynthesis (blue), biosynthesis (black)].

Ubiquitin Chains

S. N. Bavikar, L. Spasser, M. Haj-Yahya, S. V. Karthikeyan, T. Moyal, K. S. Ajish Kumar, A. Brik* _____ 758–763

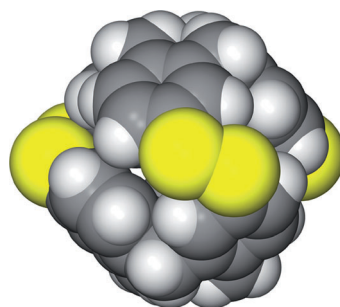


Chemical Synthesis of Ubiquitinated Peptides with Varying Lengths and Types of Ubiquitin Chains to Explore the Activity of Deubiquitinases

Adding one at a time: A general and effective synthesis yields a peptide attached to mono-, di-, tri-, and tetraubiquitin (Ub) chains (see picture for peptides with Ub and Ub₄), linked through lysine residues K48 or K63. These sets of ubiquitinated peptides were prepared in good quantities, and the activity of the enzymes UCH-L3 and IsoT with these different substrates was studied.

Host–Guest Chemistry

M. A. Little, J. Donkin, J. Fisher, M. A. Halcrow, J. Loder, M. J. Hardie* _____ 764–766

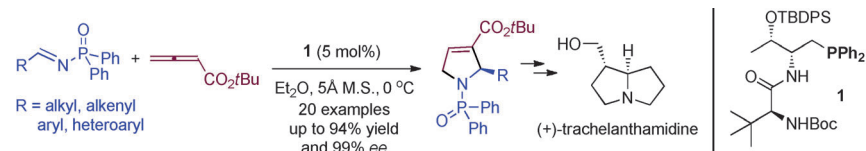


Synthesis and Methane-Binding Properties of Disulfide-Linked Cryptophane-0.0.0

Into the crypt: Direct coupling of cyclo-trithiophenolene gives a new class of cryptophane with labile disulfide linkages, which is the smallest cryptophane yet reported. The new cryptophane (see structure, S yellow, C gray, H light gray) is shown to bind methane or nitrogen in solution.

Organocatalysis

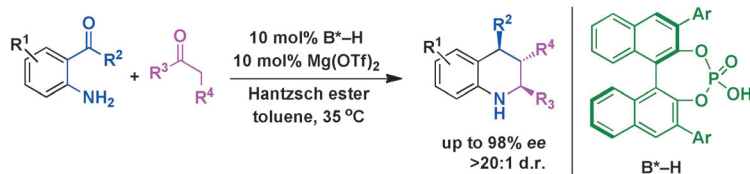
X. Han, F. Zhong, Y. Wang, Y. Lu* _____ 767–770



Versatile Enantioselective [3+2] Cyclization between Imines and Allenates Catalyzed by Dipeptide-Based Phosphines

A fast one: The title reaction proceeds in the presence of 5 mol% of the catalyst **1**, and is complete within an hour. The 2-alkyl- and 2-aryl-substituted 3-pyrroline products are obtained in good yield and with high enantioselectivity. The applica-

tion of the method to the concise formal synthesis of (+)-trachelanthamide is also demonstrated. Boc = *tert*-butoxycarbonyl, M.S. = molecular sieves, TBDPS = *tert*-butyldiphenylsilyl.



Two steps in one reaction: The title relay reaction relies on a combination of an achiral Lewis acid and a chiral Brønsted acid (B^*H in the scheme). This one-pot

method provides access to tetrahydroquinoline derivatives with multiple continuous stereogenic centers in high stereoselectivity ($>20:1$ d.r., 98% ee).

Asymmetric Relay Catalysis

L. Ren, T. Lei, J. X. Ye,
L. Z. Gong* _____ 771–774

Step-Economical Synthesis of Tetrahydroquinolines by Asymmetric Relay Catalytic Friedländer Condensation/Transfer Hydrogenation



A matter of catalyst: Azole compounds can be directly alkylated with *N*-tosylhydrazones that bear unactivated alkyl groups (see scheme; phen = 1,10-phenanthroline, Ts = *p*-toluenesulfonyl). Nickel catalysis enables the introduction

of simple secondary alkyl chains into benzoxazole compounds, whereas the alkylation of 5-aryloxazoles and benzothiazole is possible by using a cobalt catalyst.

C–H Functionalization

T. Yao, K. Hirano,* T. Satoh,
M. Miura* _____ 775–779

Nickel- and Cobalt-Catalyzed Direct Alkylation of Azoles with *N*-Tosylhydrazones Bearing Unactivated Alkyl Groups



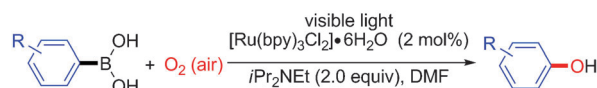
Simply the best: The title reaction has been achieved by asymmetric rhodium catalysis employing an extremely simple, chiral *N*-(sulfinyl)cinnamylamine ligand. A variety of highly enantioenriched, tertiary

α -hydroxy carbonyl derivatives were easily accessed at room temperature under mild conditions with enantioselectivities of up to 99%.

Asymmetric Catalysis

T.-S. Zhu, S.-S. Jin, M.-H. Xu* . 780–783

Rhodium-Catalyzed, Highly Enantioselective 1,2-Addition of Aryl Boronic Acids to α -Ketoesters and α -Diketones Using Simple, Chiral Sulfur–Olefin Ligands



To shed light on: The title reaction allows the generation of a variety of functionalized phenols and analogues using $[Ru(bpy)_3Cl_2] \cdot 6H_2O$ as the photocatalyst under very mild reaction conditions. This

reaction not only incorporates an oxygen atom from molecular oxygen directly into the product, but also expands the application of visible-light photocatalysis. bpy = bipyridine.

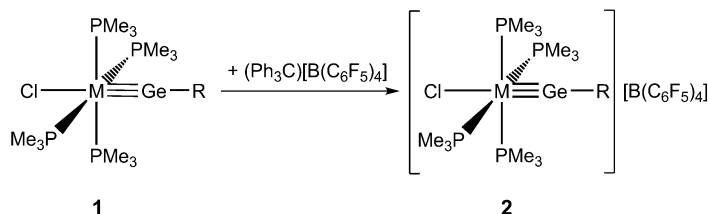
Photochemistry

Y.-Q. Zou, J.-R. Chen, X.-P. Liu, L.-Q. Lu,
R. L. Davis, K. A. Jørgensen,*
W.-J. Xiao* _____ 784–788

Highly Efficient Aerobic Oxidative Hydroxylation of Arylboronic Acids: Photoredox Catalysis Using Visible Light

Germlyidyne Complexes

A. C. Filippou,* A. Barandov,
G. Schnakenburg, B. Lewall,
M. van Gastel,* A. Marchanka 789–793



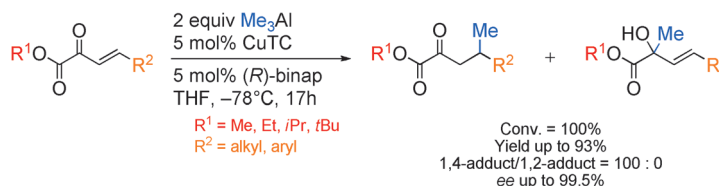
Open-Shell Complexes Containing Metal–Germanium Triple Bonds

Ge force: One-electron oxidation of the 18 valence electron (VE) germlyidyne complexes **1** provides access to the first open-shell germlyidyne complexes **2** (see scheme; M = Mo, W; R = C₆H₃-2,6-Me₂)

that are analogous to metal alkylidyne complexes. The geometric and electronic structures of the 17 VE complexes **2** were determined by a combination of experimental and theoretical methods.

Asymmetric Catalysis

L. Gremaud, A. Alexakis* 794–797



Enantioselective Copper-Catalyzed Conjugate Addition of Trimethylaluminum to β,γ -Unsaturated α -Ketoesters

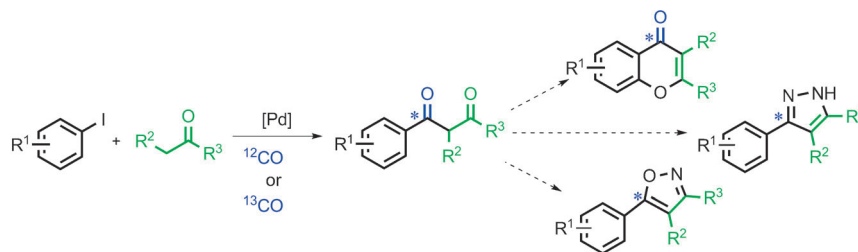
Not a cop out: The copper-catalyzed asymmetric conjugate addition of organometallic reagents to Michael acceptors is an important methodology for forming a C–C bond in an enantioselective manner.

Such an addition of Me₃Al to β,γ -unsaturated α -ketoesters is described to proceed in high yield and selectivity. CuTC = copper(I) thiophene-2-carboxylate.

Palladium Catalysis

T. M. Gøgsig, R. H. Taaning,
A. T. Lindhardt, T. Skrydstrup* 798–801

Palladium-Catalyzed Carbonylative α -Arylation for Accessing 1,3-Diketones



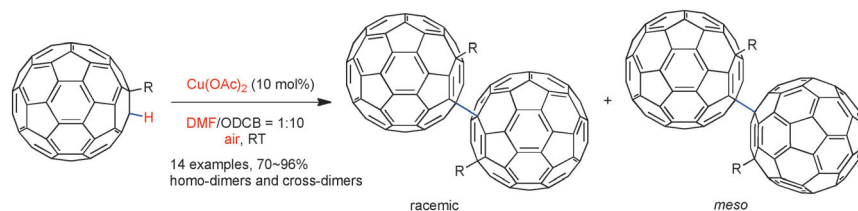
With a hint of CO: The first Pd-catalyzed carbonylative α -arylations of simple ketones with carbon monoxide is presented for the direct synthesis of 1,3-diketones (see scheme). The method uses

only stoichiometric amounts of CO, and hence allows for the simple installment of carbon isotopes into the core structures of heterocyclic compounds.

Fullerenes

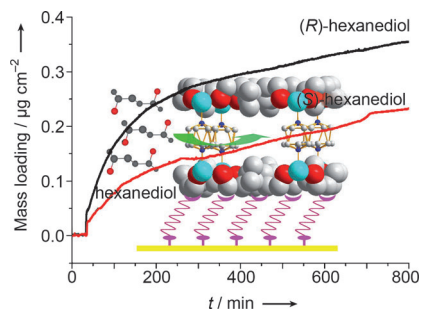
S. Lu, T. Jin,* E. Kwon, M. Bao,
Y. Yamamoto* 802–806

Highly Efficient Cu(OAc)₂-Catalyzed Dimerization of Monofunctionalized Hydrofullerenes Leading to Single-Bonded [60]Fullerene Dimers



Dimers are a girl's best friend: The title reaction allows the formation of single-bonded fullerene dimers with extremely high chemical yield and high compatibility with various functional groups, which are

highly soluble in organic solvents. The use of Cu(OAc)₂ catalyst with dimethylformamide or acetonitrile as additives under air is the critical factor in achieving the highly efficient catalytic dimerization.



Stuck on you: Preferred (110) and (001) orientation of enantiopure $[\{Zn_2((+)\text{cam})_2(\text{dabco})\}_n]$ ((+)cam = (1*R*,3*S*)-(+)-camphoric acid, dabco = 1,4-diazabicyclo(2.2.2)octane) thin films can be controlled by carboxylate and pyridyl groups on self-assembled monolayers (SAMs). With a quartz crystal microbalance, the enantioselective adsorption of enantiomeric hexanediol pairs by enantiopure surface-attached metal-organic frameworks (SURMOF) $[Zn_2((\pm)\text{cam})_2(\text{dabco})]$ pairs can be demonstrated (see picture).

Metal–Organic Frameworks

B. Liu, O. Shekhah, H. K. Arslan, J. Liu, C. Wöll,* R. A. Fischer* — 807–810

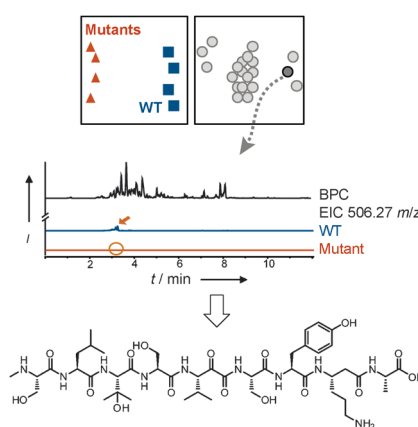
Enantiopure Metal–Organic Framework Thin Films: Oriented SURMOF Growth and Enantioselective Adsorption



Front Cover



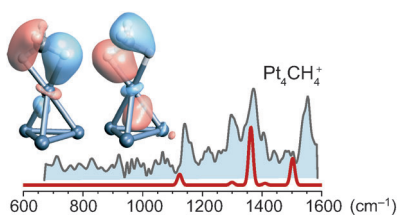
Come to the fore: The novel myxobacterial metabolite myxoprincomide is easy to overlook in the complex LC-MS data recorded for the metabolome of *Myxococcus xanthus* DK1622, such that advanced analytical techniques were needed for its discovery. By enhancing genomics-based natural products research with powerful analytical tools for in-depth metabolome mining, two additional such “hidden” metabolites have been uncovered.



Natural Products

N. S. Cortina, D. Krug, A. Plaza, O. Revermann, R. Müller* — 811–816

Myxoprincomide: A Natural Product from *Myxococcus xanthus* Discovered by Comprehensive Analysis of the Secondary Metabolome



Stretch Me–H: Methane activated by adsorption on small platinum clusters is characterized by the vibrational fingerprint of the cluster complex. The C–H bond activation is distributed over two bonds, which corresponds with a decreased activation of each of the bonds but should lead to improved control over the reactivity of methane.

Methane Activation

D. J. Harding, C. Kerpál, G. Meijer, A. Fielicke* — 817–819

Activated Methane on Small Cationic Platinum Clusters



Supporting information is available on www.angewandte.org (see article for access details).



A video clip is available as Supporting Information on www.angewandte.org (see article for access details).



This article is available online free of charge (Open Access)



This article is accompanied by a cover picture (front or back cover, and inside or outside).

Looking for outstanding employees?

Do you need another expert for your excellent team?
... Chemists, PhD Students, Managers, Professors, Sales Representatives...

Place an advert in the printed version and have it made available online for
1 month, free of charge!

Angewandte Chemie International Edition

Advertising Sales Department: Marion Schulz

Phone: 0 62 01 - 60 65 65

Fax: 0 62 01 - 60 65 50

E-Mail: MSchulz@wiley-vch.de

Service

Spotlight on Angewandte's
Sister Journals 577–579

Vacancies A3

Preview 822

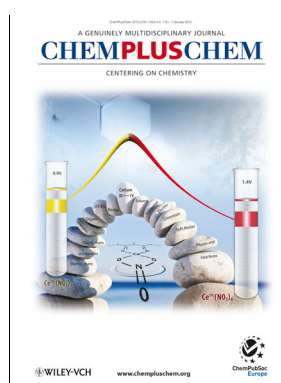
Check out these journals:



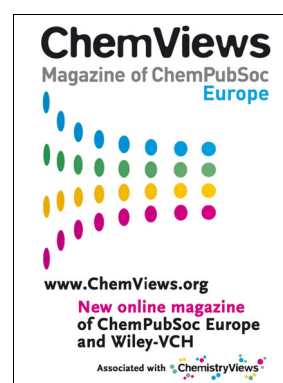
www.chemasianj.org



www.chemcatchem.org



www.chempluschem.org



www.chemviewschem.org